Genes, Brain and Behavior
Official publication of the International Behavioural and Neural Genetics Society

Genes, Brain and Behavior (2015) ***14:*** *357–368* doi: 10.1111/gbb.12217

The burrowing behavior of the nematode *Caenorhabditis elegans*: a new assay for the study of neuromuscular disorders[1]

C. Beron†, A. G. Vidal-Gadea†,*, J. Cohn, A. Parikh, G. Hwang and J. T. Pierce-Shimomura*

Department of Neuroscience, Center for Brain, Behavior & Evolution; Waggoner Center for Alcohol and Addiction Research, Center for Learning and Memory, The University of Texas at Austin, Austin, TX 78712, USA

† These authors contributed equally to this manuscript.
[1] C.B. conducted burrowing experiments, suppression screen and contributed to the writing. A.G.V.-G. contributed to all experiments, study design, and manuscript writing; J.C. performed imaging of musculature, contributed to writing; A.P. contributed to burrowing experiments; G.H. contributed to burrowing experiments; J.T.P.-S. contributed to experiments, study design and manuscript writing.

**Corresponding authors: Dr J. T. Pierce-Shimomura, Department of Neuroscience, The University of Texas at Austin, 2506 Speedway NMS 5.234, Mailcode C7350, Austin, TX 78712, USA. E-mail: jonps@austin.utexas.edu or Dr A. Vidal-Gadea, Department of Neuroscience, The University of Texas at Austin, 2506 Speedway NMS 5.234, Mailcode C7350, Austin, TX 78712, USA. E-mail: agvg75@gmail.com*

The nematode *Caenorhabditis elegans* has been a powerful model system for the study of key muscle genes relevant to human neuromuscular function and disorders. The behavioral robustness of *C. elegans*, however, has hindered its use in the study of certain neuromuscular disorders because many worm models of human disease show only subtle phenotypes while crawling. By contrast, in their natural habitat, *C. elegans* likely spends much of the time burrowing through the soil matrix. We developed a burrowing assay to challenge motor output by placing worms in agar-filled pipettes of increasing densities. We find that burrowing involves distinct kinematics and turning strategies from crawling that vary with the properties of the substrate. We show that mutants mimicking Duchenne muscular dystrophy by lacking a functional ortholog of the dystrophin protein, DYS-1, crawl normally but are severely impaired in burrowing. Muscular degeneration in the *dys-1* mutant is hastened and exacerbated by burrowing, while wild type shows no such damage. To test whether neuromuscular integrity might be compensated genetically in the *dys-1* mutant, we performed a genetic screen and isolated several suppressor mutants with proficient burrowing in a *dys-1* mutant background. Further study of burrowing in *C. elegans* will enhance the study of diseases affecting neuromuscular integrity, and will provide insights into the natural behavior of this and other nematodes.

Keywords: Behavior, burrowing, *Caenorhabditis elegans*, dystrophin, nematode

Received 24 September 2014, revised 6 April 2015, accepted for publication 7 April 2015

For over half a century, the nematode *Caenorhabditis elegans* has been successfully used to study the cellular, molecular and genetic basis of neuromuscular function and disease (Culetto & Sattelle 2000; Dougherty & Calhoun 1948). Most of this research has relied on assessing worms crawling on an agar-filled plate as the primary behavioral diagnostic of neuromuscular integrity (Hart 2006). Crawling offers an amenable behavioral readout in the study of key genes expressed in neurons and muscle. In fact, many human genes, such as distinct myosins and neurotransmitter transporters, were first identified in *C. elegans* as mutants deficient in crawling, the so-called uncoordinated (unc) phenotype (Brenner 1974; Harris & Epstein 1977; McIntire *et al.* 1997). However, *C. elegans* appears less suited to study phenomena like muscular dystrophy (MD) where the neuromusculature of animals is not significantly challenged by the relatively facile task of crawling on an agar surface. Indeed, previous studies have struggled to identify severe phenotypes in worms modeling MD by carrying loss-of-function mutations in the *C. elegans* dystrophin ortholog, *dys-1*, responsible for Duchenne muscular dystrophy (DMD). The *dys-1* mutant displays only moderate behavioral phenotypes, such as a slightly crooked neck; however, the *dys-1* mutant can crawl normally (Giugia *et al.* 1999). This unpairing of genotype and phenotype is not only found in the worm model of the disease. Indeed, fly (Shcherbata *et al.* 2007) and mouse (Durbeej & Campbell 2002; Torres & Duchen 1987) systems that model DMD through disruption of dystrophin also have failed to model the extreme behavioral phenotype observed in humans. Many groups working on worms (e.g. Gieseler *et al.* 2000; Mariol & Ségalat 2001), flies (e.g. Kucherenko *et al.* 2008), and mice (Deconinck *et al.* 1997) have thus turned to study sensitized strains in an attempt to recapitulate the human phenotype. However, genetic sensitization may limit the applicability of results to MD that occurs in humans with mutations only in dystrophin (Monaco *et al.* 1986).

The lack of acute behavioral phenotypes in these models may be a result from compensatory pathways (Michele

et al. 2002; Moore *et al.* 2002) or alternatively, it may be the product of the behavioral paradigms used to evaluate function. Petrof *et al.* (1993) showed that the degree of muscular degeneration in DMD^{mdx} mice was directly correlated with the strength (and not the frequency) of muscle contraction. To investigate if behavioral paradigms exposing *dys-1* worms to increased strength of muscular exertion could better recapitulate the ethology of DMD, we set out to study burrowing in worms. As a prelude, we provide an initial description of the kinematics of the burrowing behavior of *C. elegans*, and compare burrowing to crawling and swimming behaviors. We then investigate the potential usefulness of burrowing as a diagnostic of neuromuscular integrity by comparing muscular degeneration in *dys-1* animals reared in a burrowing vs. a crawling regiment. Lastly, we use this behavior to perform the first behavioral suppression screen on worms modeling MD.

Materials and methods

Animals

Caenorhabditis elegans strains wild-type N2, *dys-1(eg33)*, *islo1(eg978)*, and *dys-1(cx18)* were obtained from the *Caenorhabditis* Genetic Center or were gifts from Dr Hoky Kim. Oh and Kim (2013) report that the *eg33* allele has a nonsense mutation at position 3287, and that the *cx18* allele has a nonsense mutation at position 2721. Animals were cultured on nematode growth media (NGM) agar plates and fed OP50 strain *Escherichia coli* at 20°C as described (Brenner 1974). Wild-type and *dys-1* mutant worms expressing nuclear and mitochondrial GFP in body wall muscles were the HKK5 and HKK22 strains as previously described (Oh & Kim 2013). Mitochondria and nuclei in the muscles were labeled with green fluorescent protein via the integrated transgene array *ccIs4251[P$_{myo-3}$GFP-NLS, P$_{myo-3}$ GFP-mit]* (Oh & Kim 2013). Out of the four different *dys-1* suppressor mutant strains isolated in this study, JPS518 was the only one that successfully mated with the *dys-1;ccIs4251* strain allowing us to analyze its subcellular muscle integrity. The *dys-1* gene was knocked down via RNA interference as originally described (Timmons & Fire 1998).

Behavioral analyses

Adult (day 1) animals were picked into a 1-μl droplet of NGM buffer (Hart 2006). A glass capillary was used to transfer by injection the worms into a 1.5-ml glass pipette prefilled with agar of 0.5%, 1.5%, 3%, 6%, or 9% densities in chemotaxis buffer (Hart 2006). Following a 2-min acclimation period, 10 worms in each condition were filmed for 5 min at 10 frames/second, 344 pixels/mm using a Flea2 camera (Point Grey Research, Richmond, Canada) mounted on a dissecting microscope and using StreamPix3 software (NorPix, Montreal, Canada).

Burrowing proficiency

Worms were injected into one end of a 10-ml plastic pipette and sealed with Parafilm wax. The opposite end of the plastic pipette had an attractant, diacetyl, to encourage directed burrowing. To quantify proficiency at burrowing, we counted the number of worms on either side of the 4-cm mark. The majority of wild-type worms migrate past this position (Fig. 4d). Worms did not make sufficient progress toward the opposite side without the attractant.

Single worms

Animal midlines (13 points) of single worms were derived as previously described using a custom image analysis algorithm available upon request (Pierce-Shimomura *et al.* 2008) (ImagePro; Media Cybernetics, Rockville, MD, USA). The series of 11 angles formed by the midline was represented in a color-coded 'curvature column' (Fig. 1b). A time series of curvature columns formed a 'curvature matrix' in which blue and red stripes represent the waves of dorsal and ventral curvature, respectively, passing along the body. Curvature matrices and average phase cycles were obtained and plotted using IgorPro (Wave Metrics, Lake Oswego, OR, USA). The quality of each digitized worm midline was manually checked, superimposing it on the original video frame, and corrected if necessary for every video frame used in this study. For each condition, 10 worms were used.

Groups of worms

For parameters listed below, we analyzed the behavior of groups of 10 worms confined within a square copper frame (1.4 cm per side) on a blank NGM agar plate, which was recorded as before (Vidal-Gadea *et al.* 2012). Worm centroids were detected and tracked using ImagePro. For each condition, three assays containing 10 worms each were conducted ($N = 30$). Worms were filmed for 3 min following a 2-min acclimation period to the arena consisting of a copper frame fused to the agar surface to contain the worms.

Parameters measured

Head-bend frequency

Measured using the time required for 10 consecutive, and uninterrupted, head bends.

Velocity

Distance traveled in 1 min by body centroid in the direction of locomotion.

Turning rate

Number of direction changes per minute.

Reversals

Consist of changes in forward trajectory preceded by reversed locomotion.

Omega bends

Changes in trajectory produced by a single full ventral bend where the anterior and posterior ends of the animals come in proximity adopting a shape reminiscent of the Greek letter naming the maneuver (Ω).

Deep bends

Changes in trajectory produced by a single body bend of large amplitude.

Lateral bends

Consist of changes in trajectory orthogonal to the plane of locomotion produced by a laterally directed deep bend.

Chemotaxis

Worms were assessed for chemotaxis performance according to Bargmann and Horvitz (1991).

Suppressor screen

We conducted our suppressor screen according to the protocol described by Jorgensen and Mango (2002) but using 3-μM *N*-ethyl-*N*-nitrosourea as the mutagen. Approximately 100 haploid genomes were screened by re-plating the progeny of 50 mutagenized F1 worms. To make sure that food was available to worms in the pipettes, we centrifuged 1.5 ml of OP50 liquid culture and pipetted half of each pellet 5 cm away from the start point, and the other half 10 cm away from the start point.

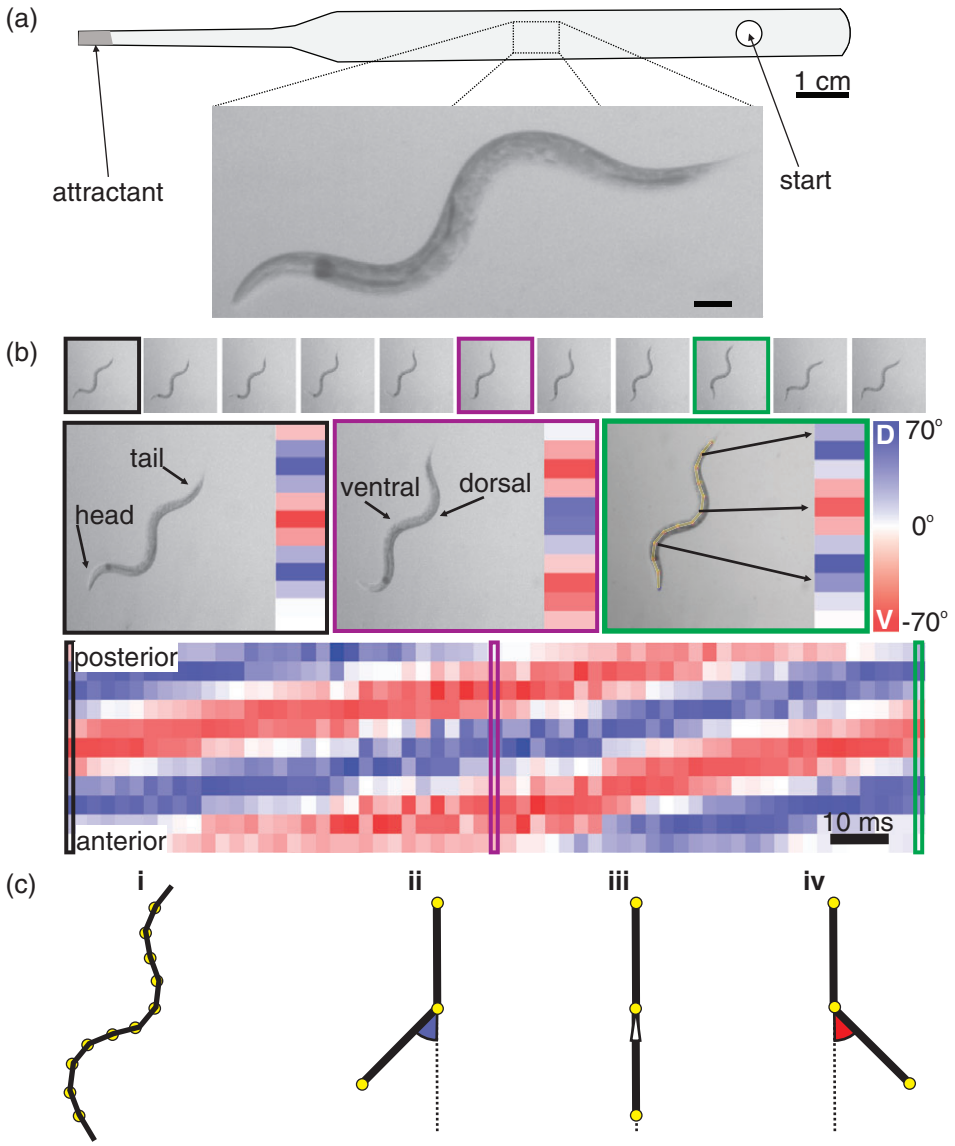

Figure 1: Kinematic analysis of the burrowing behavior of *C. elegans*. (a) We used 1.5-ml glass pipettes filled with agar of varying densities to film the burrowing behavior of individual worms. Adults were injected into one end of the pipette and filmed as they burrowed to an attractant (diacetyl) placed at the opposite end (inset). (b) Our custom algorithm implemented in ImagePro detected and digitized worms while freely behaving (top). The midline of animals were then divided into 11 sections of equal length (middle) and the angle between these was measured and assigned a color ranging from red for 70° ventral, to white for 0°, to blue for 70° dorsal. Here a burrowing worm is shown. Three color-coded frames are followed through the spinning process, which results in the creation of a behavioral matrix that describes the entire behavior of the animal over time (bottom). (c) A spined worm is shown (i) to illustrate the angles represented in the curvature matrix. A dorsal angle is presented as a shade of blue (ii), straight angles appear as white (iii), and ventral angles as shades of red (iv). In this and all curvature matrices, anterior is down and posterior is up.

Imaging and analysis

Worms were removed from the burrowing pipettes by ejecting the agar and immersing in NGM liquid. This allowed the recovery of worms with motor deficits. After recovery, animals were mounted onto 2% agar pads containing 30-mM sodium azide. Optical stacks were acquired using a Zeiss 710 Laser Scanning Confocal Microscope connected to a fluorescent light source. Images were processed using ImageJ 1.48 (NIH, Bethesda, MD, USA) software. Although we observed muscle degeneration throughout the worm, we focused our analysis on the midbody and posterior half of the animal because of the simpler muscle structure.

Statistical analysis

Sigmaplot 12.5 was used for all statistical analyses to determine significance ($P \leq 0.05$, two tailed) between two or more groups. If the

groups being compared passed the Shapiro–Wilk normality test, they were analyzed using standard *t*-test or analysis of variance (ANOVA) test where appropriate. Groups that failed to pass the normality or equal variance test were compared using Mann–Whitney Sum of Rank tests. In every figure means and SEM are reported.

Results

Development of a novel burrowing assay

To study the kinematics of burrowing behavior for individual *C. elegans*, we used agar-filled pipettes (Fig. 1a). We injected a liquid solution of worms into the agar 1 cm away from one end of the pipette. We then filmed worms while they burrowed toward a drop of the attractant diacetyl placed on the opposite end of the pipette. We manually adjusted the pipette to film worms, adjusting the focal plane and repositioning the pipette as necessary to keep them in view.

Burrowing kinematics were obtained by using a custom-built algorithm (Pierce-Shimomura *et al.* 2008) that divided the midline of the worm into 11 equal segments and plotted the measured angles between successive segments (Fig. 1b). In this way, the entire behavior of the animal could be analyzed and displayed for comparison as a color-coded matrix where the extent of dorsal and ventral flexion are correlated with the intensity of the blue and red color, respectively (Fig. 1c). Video segments were analyzed only if the worm maintained its dorsoventral bending along the focal plane of the video camera.

Burrowing kinematics are distinct from swimming and crawling kinematics

Caenorhabditis elegans locomotes forward by propagating dorsoventral bends down the length of their bodies from anterior to posterior. We found that the frequency of head bends during burrowing was lower than the frequency during crawling and swimming over the range of agar densities tested (between 0.5% and 9%, Fig. 2a). Head-bend frequency displayed a bell-shaped curve with agar density. This might be explained by different forms of movement across agar densities. Worms appeared to primarily exhibit a form of motion resembling 'slow crawling' in agar less dense than 1.7%. For denser agar conditions, however, worms appeared to adopt a distinct 'burrowing' form of motion described in more detail below. Note that even the lowest density gel (0.5% provided significantly more resistance than water. The head-bend variability observed through the range of substrate densities (reported as SEM in Fig. 2a) was substantially smaller for burrowing than for swimming or crawling.

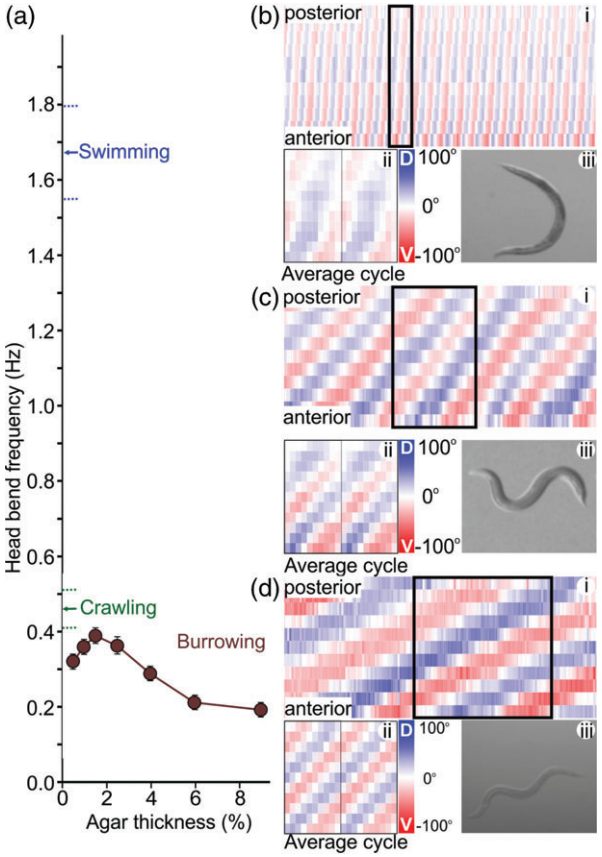

Figure 2: Burrowing is distinct from swimming and crawling behaviors. (a) Burrowing head-bend frequency in a range of agar densities was lower than crawling frequency (mean and SEM shown in green), and swimming (mean and SEM shown in blue). $N = 15$ worms, 10 head bends each, for swimming and crawling, and $N = 10$ worms, 10 head bends each, for each agar density during burrowing. (b) Curvature matrix plot of a representative swimming bout 10 seconds long (i). The phase plot of matrix data averaged across individual head-bend cycles (ii) shows how the worm switches from a ventrally bent 'C' shaped posture, pictured on the right (iii), to a dorsally bent C-shaped posture and back. (c) Crawling worms moved by means of a persistent but propagating 'S' shape (i), as depicted by the average cycle plot (ii) and picture (iii). (d) Across densities, worms burrowed with a continuous 'M' (or 'W') shape. Burrowing is also distinct from swimming and crawling in lacking the dampening of posteriorly directed bends. All curvature matrices are 10 seconds long. $N = 10$ worms with minimum of 10 cycles each for every condition, representative examples shown.

Qualitative differences in burrowing kinematics

Aside from their decreased bend frequency, burrowing was also kinematically distinct from crawling and swimming. Across behaviors, bending amplitude (represented by the depth of the blue and red colors in the matrix plots) appeared inversely related to bending frequency (Fig. 2bi–di). Average maximal neck bend amplitudes were $28.4 \pm 3.11°$ SD for crawling, $75.3 \pm 10.1°$ SD for swimming and $88.7 \pm 3.2°$ SD for burrowing ($n = 8$ each). Swimming and crawling exhibited posterior dampening of the propagated bend, a phenomenon where the amplitude of the body bend is greatest near the head and gradually dampens as it reaches the tail (Fig. S1, Supporting Information). This is evident on the representative curvature matrices and average cycle plots as the darker blue and red at the bottom (anterior) of the plots when compared with the lighter colors at the top (posterior) (Fig. 2bi and ii, 2ci and ii). It is also evidenced when plotting neck and

tail curvature time series and computing the average change in maximal bend (Fig. S1). By contrast, burrowing worms did not exhibit as significant dampening of bends (Fig. 2di and ii; Fig. S1). The average cycle plots (ii) and the accompanying screen shots (iii) also illustrate the distinct shapes worms assume in each behavior. Swimming animals can be said to locomote by alternating dorsal and ventral 'C'-shaped body postures, while crawling and burrowing rely on persistent 'S' and 'W' shaped postures, respectively (Fig. 2biii–ciii). This is evident after noting that most columns in the curvature matrices include two changes in color for crawling, and always at least three changes for burrowing. By contrast, the dorsal and ventral C-shaped postures during swimming are apparent as curvature columns with only red or blue coded colors at the beginning and middle of each head-bend cycle.

Worms modulate their turning strategies according to their environment

While migrating toward or away from a stimulus, *C. elegans* has several ways to alter their trajectory (Croll 1975; Iino & Yoshida 2009; Pierce-Shimomura *et al.* 1999; Ward 1973). Worms can perform a reversal, which consists of one to several bends that propagate from tail to head before a forward change in direction. During an omega bend, the worm bends its head ventrally to touch its posterior end, causing its body to form an Ω shape, before heading in the opposite direction. Deep bends are changes in trajectory produced by single bends of increased amplitude, resulting in a new anterior-directed heading.

We found that while swimming worms changed direction primarily by using omega and deep bends, crawling worms relied heavily on reversals (Fig. 3a), consistent with our previous report (Vidal-Gadea *et al.* 2012). Burrowing worms modified their turning strategy according to the density of the substrate (Fig. 3a,b). At low densities, burrowing worms used all strategies also used during swimming and crawling together with an additional turning strategy that we defined as lateral bends (see Video S1). During a lateral bend, the worm changes direction by virtue of a single left or right bend that causes the worm to now travel in an orthogonal plane to their ongoing dorsoventral movement. Like reversals and deep bends, lateral bends were observed for animals burrowing at densities below 3%. Above this density animals relied almost entirely on omega bends.

Worms modeling MD are impaired at burrowing

To determine if the burrowing behavior could be used as a readout of neuromuscular integrity, we compared the burrowing and crawling abilities of wild-type worms to that of two strains carrying loss-of-function mutations in the *dys-1* gene. The *dys-1* gene is orthologous to the human dystrophin gene responsible for DMD when mutated. We were motivated to test the burrowing ability of the *dys-1* mutant because previous reports found that they were grossly normal in crawling (Giugia *et al.* 1999). Consistent with this, we found that both *dys-1* mutant strains showed no deficit in crawl frequency

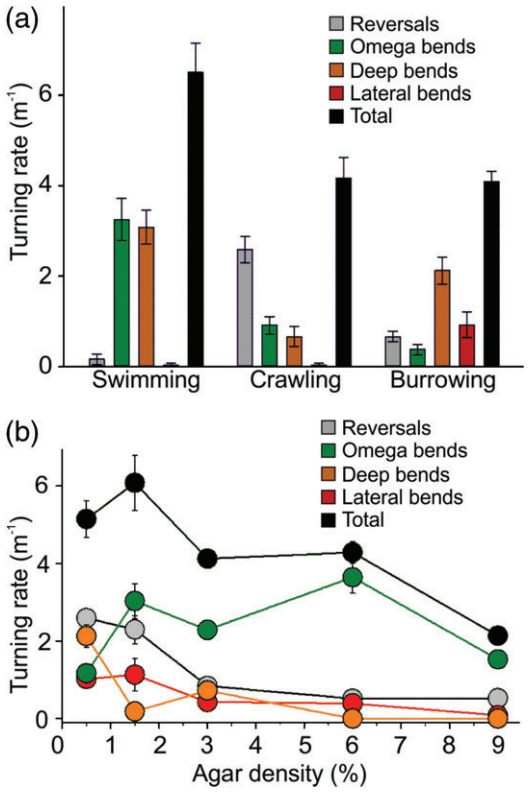

Figure 3: Worms alter their trajectory by different means depending on substrate properties. (a) Wild-type worms showed distinct strategies to change their direction depending on their environment. Swimming animals changed direction by producing deep bends and omega bends. Crawling worms favored reversals and burrowing worms rely on deep and lateral bends. (b) As substrate density increases, worms decreased their turning rate and relied increasingly on omega bends. At lower densities, however, worms used several turning strategies including lateral bends characterized by three-dimensional waves. Mean and SEM reported for 3-min observation period after 30-min of acclimation for 30 worms in each condition.

(Fig. 4a). Their rate of reversal and crawling velocity also appeared unimpaired (Fig. 4b,c).

To compare the burrowing ability of different strains, we injected worms into 5-ml agar-filled plastic pipettes and allowed the worms to burrow toward an attractant for 2 h (Fig. 1a). After this time, worms were scored according to their progress along the chemoattractant gradient (Fig. 1b). In contrast to their proficient crawling, both of the *dys-1* strains were severely impaired at burrowing (Fig. 4d, $U = 0.000$, $P < 0.001$ for WT vs. both *cx18* and *eg33*). Individual *dys-1* mutants often exhibit periods of immobility as apparent as static pattern in the curvature matrix (Fig. 4e, bottom, Video S2). When moving, however, individual *dys-1* mutants burrowed using kinematics reminiscent of crawling. Bends were faster, more variable in amplitude, and dampened posteriorly (Fig. 4e, middle) compared with wild-type burrowing (Fig. 4e, top).

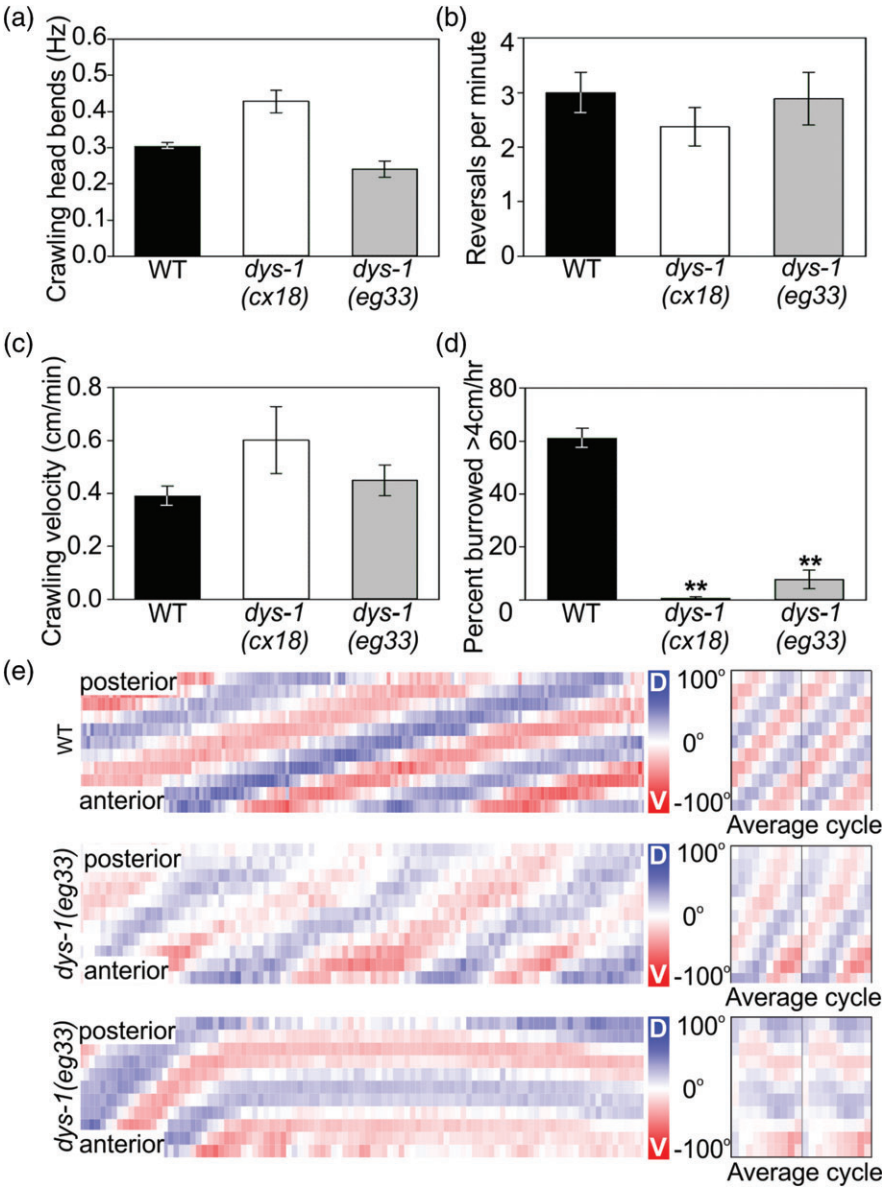

Figure 4: Burrowing is an ideal behavior to assess neuromuscular integrity. We tested two *dys-1* loss-of-function alleles that model DMD. Crawling behavior failed to produce striking phenotypes for these animals. For example, *dys-1* worms display no defect in head-bend frequency (a), reversal rate (b) and velocity (c) when crawling. The same *dys-1* mutant strains, however, were severely impaired in burrowing (d). Mean and SEM reported for samples of 30 worms for the crawling, and 65 animals for the burrowing experiments. $^{**}P < 0.001$ two-tailed *t*-test. (e) Unlike wild-type (top) mutants, burrowing *dys-1* mutants had crawl-like kinematics (middle) interspersed with periods of immobility (bottom) as evident in the curvature matrices (10 seconds each). Average curvature plots for corresponding strain on right.

Because *dys-1* is expressed in both muscles and neurons, inefficient burrowing of the *dys-1* mutant might be explained by a neuronal deficit in sensing the attractant and/or orienting toward the attractant. However, we found that the *dys-1* mutant readily performed chemotaxis when crawling in a standard assay (Fig. S2a). In addition, to confirm that the burrowing defect reflected a loss of *dys-1* function, we assayed how knock-down of *dys-1* via RNA interference affected burrowing. We found that compared with control-treated worms, *dys-1*-RNAi-treated worms were profoundly defective in burrowing (Fig. S2b). Lastly, we tested whether the burrowing defect extended to additional members of the Dystrophin Glycoprotein complex in *C. elegans* muscle, by assaying the mutant *islo-1*. The ISLO-1 protein physically links DYS-1 to the highly conserved BK potassium channel throughout muscle to preserve calcium activation of the channel (Kim *et al.* 2009). We found that the *islo-1* mutant was similarly defective in burrowing but not crawling like the *dys-1* mutant (Fig. S3).

Taking the above results together, we conclude that the *dys-1* gene is likely required for proper muscle function and for efficient burrowing.

Burrowing increases the rate and extent of muscular degeneration in animals modeling MD

Work on mouse models of DMD suggests that the extent of muscular degeneration directly correlates with the strength of muscle contractions (Petrof *et al.* 1993). Crawling *dys-1* mutant worms show normal muscle morphology in young adulthood, with a small subset of seemingly random muscle

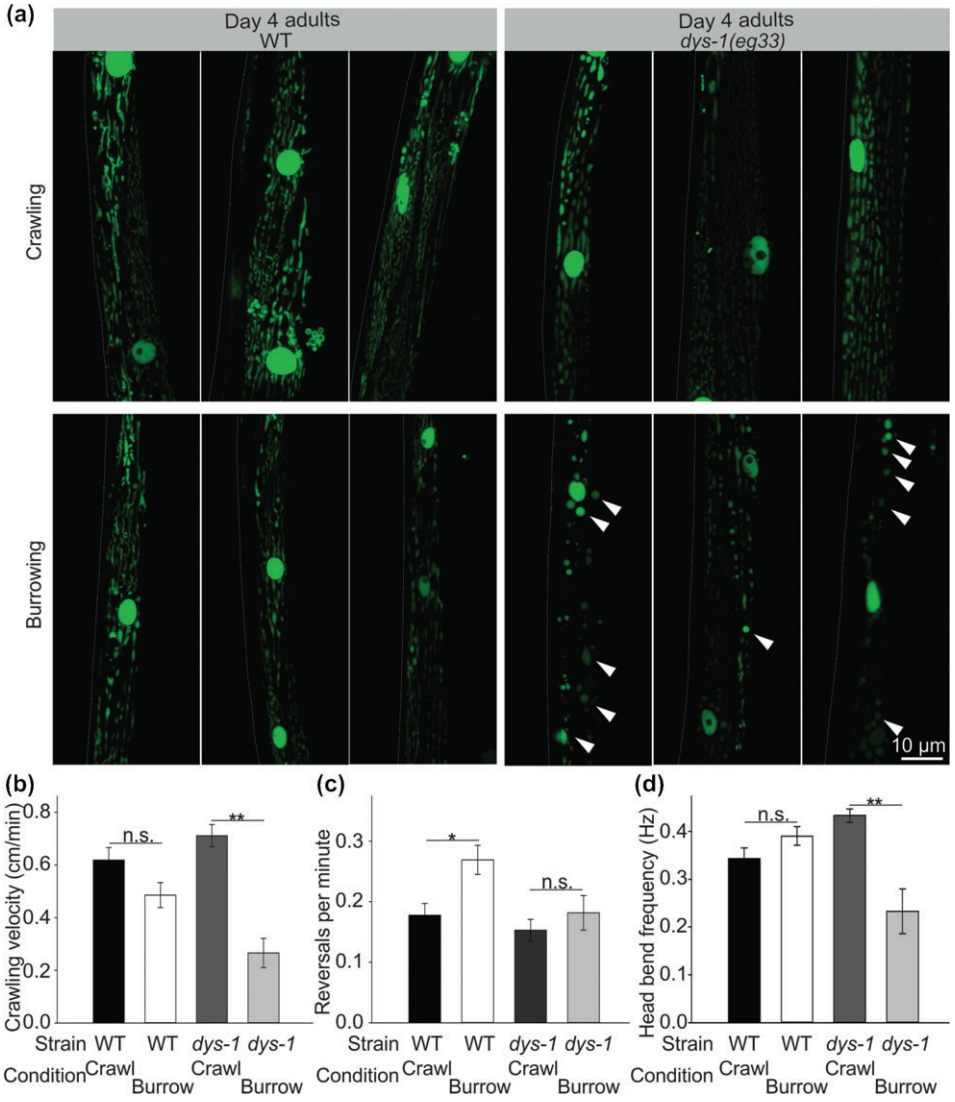

Figure 5: Burrowing hastens muscular degeneration in worms modeling MD. Young (L4) wild-type and *dys-1* mutant worms expressing GFP-tagged muscle nuclei and mitochondria (*ccIs4251*[$P_{myo\text{-}3::}$*GFP-NLS* + $P_{myo\text{-}3::}$*GFP-mit*]) were grown on either agar plates with bacteria, or in 6% agar pipettes with bacteria at opposite and half-way points to force animals to crawl or burrow, respectively. After 4 days, crawling ability was tested and their musculature was subsequently imaged. Wild-type and *dys-1* mutant worms showed only limited muscle degeneration when raised in the crawling condition ((a) top row); however, *dys-1* mutants showed marked muscular degeneration when raised in the burrowing condition ((a) bottom row). Arrowheads point to areas of accumulation of GFP, indicative of muscle cell degeneration. Three representative worms are shown for each condition. The muscular degeneration observed for burrowing *dys-1* mutants was reflected in their locomotor dysfunction. (b) *dys-1(eg33)* mutant worms raised in the burrowing condition showed a marked decrease in crawling velocity compared with their sisters raised in the crawling condition. (c) Although an increase in reversal frequency might be associated with the measured decrease in velocity for wild type, this was not the case for *dys-1* mutants. Instead, decreases in *dys-1* crawling velocity seemed to be related to lower bending frequency (d). Here we report the mean and SEM for $N = 30$ worms for each condition. $^{**}P < 0.001$, two-tailed *t*-test.

cells dying only after advanced age (>10 days, Oh & Kim 2013). We hypothesized that muscle degeneration may be more readily observed in the *dys-1* mutant if its muscles were challenged by forcing worms to burrow rather than to crawl (as they do under standard culture conditions). We raised wild-type and *dys-1* mutant worms in conditions where they were required to obtain food by crawling (standard conditions) or by burrowing (similar to described above). Specifically, we placed 20 young (day 3, L4-larval stage) wild-type and *dys-1* mutant worms on agar plates seeded with bacterial lawns for standard conditions, and inside 6% agar-filled pipettes also seeded with bacterial food at regular

intervals. Both wild-type and *dys-1* strains carried integrated GFP transgenes to label muscle nuclei and mitochondria to observe muscular integrity after being raised in each condition.

After 4 days, adult worms were retrieved from crawling or burrowing conditions and assessed for muscular and behavioral integrity (Fig. 5). Although some degeneration was seen on *dys-1* mutants grown in plates, as reported previously (Oh & Kim 2013), *dys-1* mutants forced to burrow in pipettes showed extensive muscle cell degeneration. This was evident by the loss of distinct circular appearance of GFP-labeled muscle cell nuclei, the absence of clearly linear arrangements of GFP-labeled mitochondria, together with the development of small aggregates of GFP indicating cell degeneration (representative confocal stack images, Fig. 5a).

As a complementary method to assess muscular integrity, same-age (day 4) worms reared in the burrowing condition were allowed to exit the pipette and crawl on an agar plate. Paralleling our imaging results of muscle cell integrity, we found that *dys-1* worms from the burrowing condition showed a marked reduction in crawling velocity when compared with wild-type worms under the same treatment (Fig. 5b, $U = 195$, $P < 0.001$ vs. $F_{59} = 1.98$, $P = 0.052$, respectively). While a modest reduction in overall crawling velocity could perhaps be attributable to an increased rate of reversals in wild type ($U = 285$, $P = 0.008$), this was unlikely to be the case for the *dys-1* mutants (Fig. 5c, $U = 625$, $P = 0.658$). Instead, the decreased crawl velocity may be explained by a reduced rate of head bends during crawling (Fig. 5d, WT: $F_{38} = 1.58$, $P = 0.123$ vs. *dys-1*: $U = 99.5$, $P = 0.001$). We conclude that burrowing presents an appropriate behavioral paradigm to evaluate the neuromuscular integrity of wild-type and neuromuscularly impaired animals.

Development of a suppressor screen for MD

The strong behavioral and anatomical phenotypes obtained from our burrowing assay led us to develop a genetic screen to search for mutations capable of suppressing the burrowing deficit of *dys-1* mutants (Fig. 6). In brief, the screen consisted of exposing *dys-1(eg33)* mutant worms to a mutagen to induce random mutations in their gametes. We assessed approximately 100 individual F2 progeny of 50 mutagenized F1 worms suggesting coverage of 100 haploid genomes. Any individual that could burrow through 1.5% agar at wild-type level by burrowing more than 10 cm in 3 h (thus suppressing the *dys-1* phenotype) was re-tested to confirm the heritability of the phenotype, and then isolated for further characterization (Fig. 6a).

Isolation of MD suppressor mutants

Our suppressor screen produced four independently derived mutants with an improved ability to burrow compared with the *dys-1(eg33)* mutant background strain (Fig. 6b). For instance, although only 5% of *dys-1* mutants could burrow more than 4 cm away from the start (*dys-1* compared with WT: $U = 0.00$ $P < 0.001$), between 50% and 55% of the four suppressor mutants (JPS515, JPS516, JPS517 and JPS518) could burrow this distance (Fig. 6b, *dys-1* compared

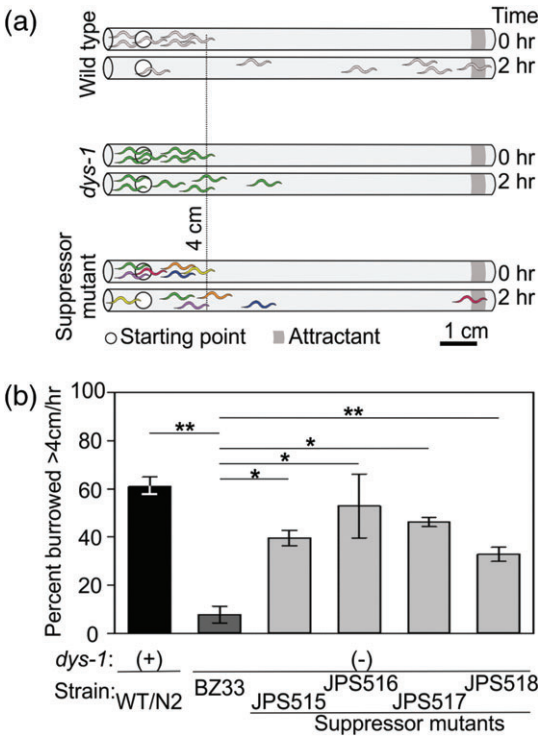

Figure 6: Suppression screen to identify mutations capable of rescuing the defective burrowing phenotype of worms modeling MD (*dys-1(eg33)* strain BZ33). (a) We devised a genetic screen to identify mutations capable of suppressing the poor burrowing ability of *dys-1* mutant. A 2-μl drop of the attractant 1:100 diacetyl diluted in ethanol was placed on one side of a 3% agar-filled pipette. After 24 h, worms were injected 20 cm away from the attractant and allowed to burrow within it. After 2 h, most wild-type worms will have migrated more than 4 cm toward the attractant (top). During the same time course, *dys-1* mutants fail to make progress toward the attractant (middle). We mutagenized *dys-1(eg33)* worms and selected animals whose *dys-1* phenotype had been suppressed by newly acquired mutations (bottom). (b) Four strains of suppressor mutants were isolated (JPS515, JPS516, JPS517 and JPS519), which displayed an improved ability to burrow over their *dys-1* background.

with JPS515: $U = 0.00$, $P = 0.006$; JPS516: $U = 1.5$, $P = 0.012$; JPS517: $U = 0.00$ $P = 0.006$; and JPS518: $U = 10$, $P < 0.001$). Each of these strains was tested for their burrowing ability on at least three separate occasions producing the same result each time.

To gain insight into neuronal and/or muscular basis of the suppression, we performed additional analysis on their crawling behavior. We found that while one strain, JPS518, appeared hyperactive in its crawling velocity (Fig. 7a), and its rate of reversals while crawling (Fig. 7b), it displayed normal head-bend frequency during crawling (Fig. 7c). Interestingly, the remaining three suppressor strains performed all these crawling behaviors at wild-type levels.

To understand how suppressor mutations enabled proficient burrowing in the *dys-1(eg33)* mutant background, we

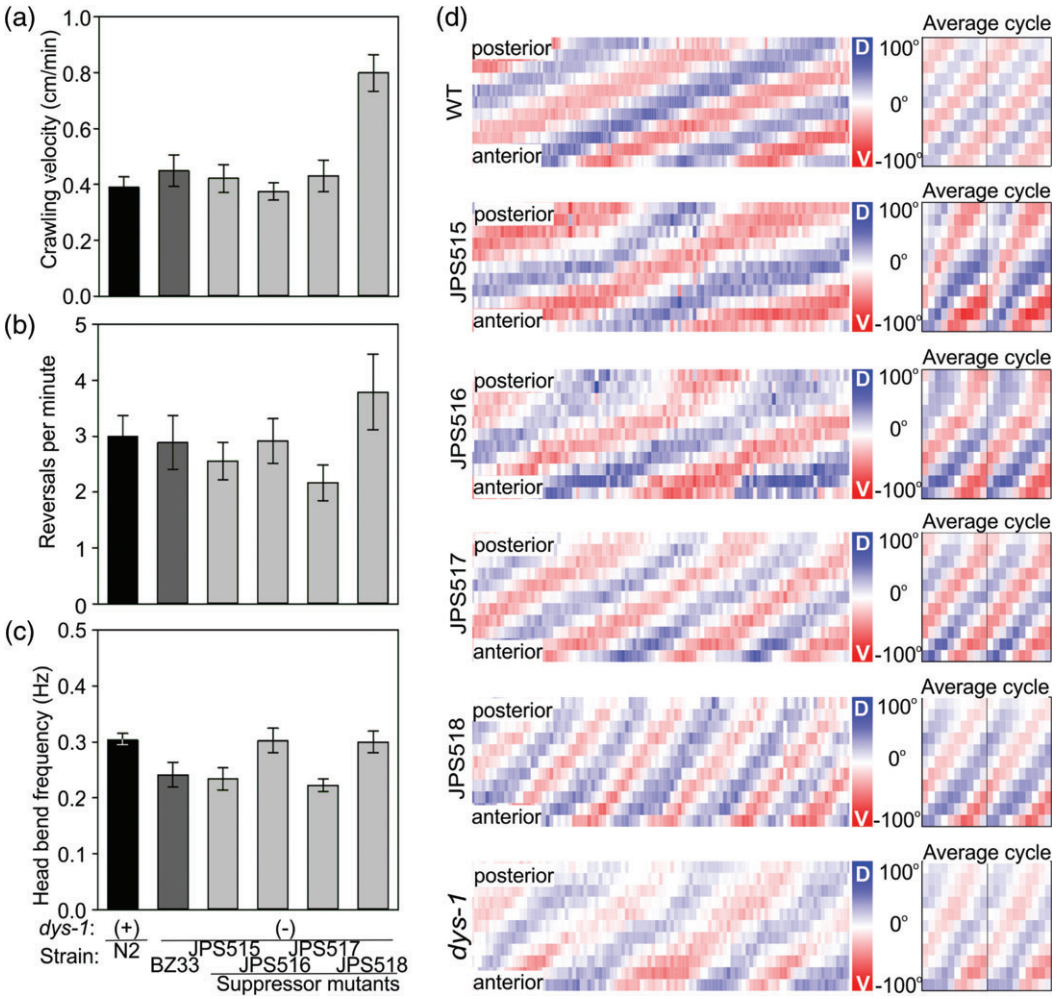

Figure 7: Behavioral characterization of suppressor mutants. Like the *dys-1(eg33)*-mutant strain BZ33, most suppressor mutants carrying the *dys-1* mutation displayed wild-type crawling velocity (a), reversal rates (b), and head-bend frequencies (c). (d) We next compared their detailed burrowing kinematics to those of wild type (top), and *dys-1* mutant worms (bottom) with curvature matrices. Suppressor mutants had kinematics reminiscent of both wild-type and *dys-1* worms. All bars show the mean and SEM of 100 animals (in five trials) for burrowing, and 15 animals for crawling (30 for *dys-1(eg33)* vxJPS518). Burrowing bouts of 10 seconds in duration are shown, alongside average phase plots (right). Anterior is at the bottom, and posterior at the top.

analyzed their burrowing behavior in more detail. In general, we found that the burrowing kinematics for these suppressor strains was intermediate between that of wild-type and *dys-1* mutant worms (Fig. 7d top and bottom, respectively).

To begin to assess if improved burrowing ability correlated with improved muscle integrity, we crossed the JPS518 mutant with the *dys-1(eg33)* strain with labeled muscle mitochondria and nuclei to determine the extent of muscular degeneration caused by burrowing in this suppressor strain (Fig. 8). The JPS518 strain was tested first simply because it was the most proficient at mating among the different suppressor strains. We found that the behavioral rescue of the burrowing phenotype in the JPS518 strain was accompanied by a decrease in muscular degeneration. To quantify the extent of degeneration, we analyzed the number of gfp-labeled nuclei in muscles throughout the posterior half of worms (Fig. S4; 5–9 animals per group). In comparison with wild type (6.33 ± 0.08), the *dys-1* mutant had a significantly smaller number of nuclei (4.66 ± 0.49) at the midbody. By contrast, the JPS518 suppressor strain had more muscle nuclei (5.66 ± 0.23) at the midbody than the *dys-1* mutant. In addition, and although not investigated here, burrowing JPS518 worms also appeared to have brighter mitochondrial GFP label when compared with crawling animals (Fig. 8).

Discussion

Although the selection of *C. elegans* as a model organism was not made on the basis of its behavioral repertoire,

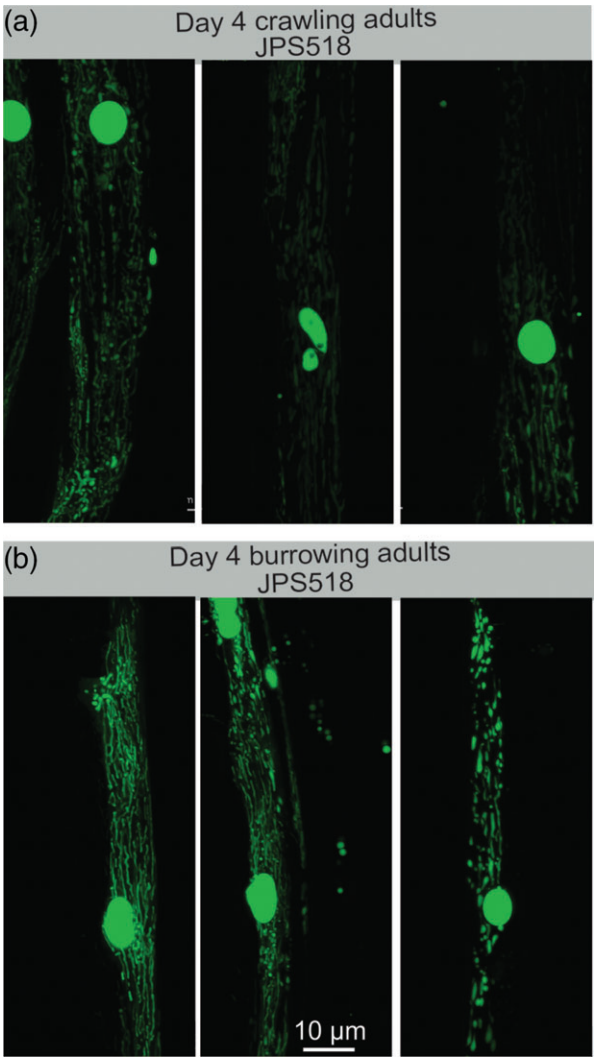

Figure 8: Suppressor mutation that improved burrowing ability also improved muscle integrity of the *dys-1* mutant. Muscle degeneration that is normally exacerbated by burrowing conditions in the *dys-1* mutant background was suppressed with the suppressor mutant strain JPS518. Note the wild-type-like pattern of GFP-labeled muscle mitochondria and nuclei from confocal stack images in both crawling and burrowing-raised conditions. Scale bar for all representative images at the bottom.

decades of research have made it evident that this compact animal is capable of a wide array of interesting behaviors. Historically, crawling has been used as a behavioral readout to elucidate the normal function of muscle and neuronal genes as well as to model human neuromuscular diseases (Kaletta & Hengartner 2006). While crawling is experimentally amenable, it is best suited for the assessment of neurological phenotypes where the timing or performance of a behavior is under neural control. The artificially facile media over which animals crawl result in worms that are able to crawl even when severely challenged by mutation or transgene. As exemplified by our *dys-1* results (Fig. 4), crawling is not an effective paradigm to distinguish subtle muscular phenotypes, where the musculature is challenged, as it is with neurological phenotypes. Using the burrowing assay developed here, we are now able to assign a strong motor phenotype to worms modeling MD, even when these mutant worms are capable of near normal crawling (Fig. 4).

The physical challenge posed by media of higher densities was evidenced by the lower frequency and variability observed for burrowing worms when compared with crawling or swimming ones (Fig. 2a). The increase in bend amplitude and the lack of posterior dampening of propagated bends further support the idea of an increased challenge to locomote in burrowing animals (Fig. 2d and Fig. S1). As the density of the media increased, worms altered their turning strategy (Fig. 3). Indeed, previous work on burrowing polychaetes showed that these annelids change their burrowing strategy with substrate density (Dorgan 2008).

The increased muscle degeneration observed in *dys-1* mutant worms under the burrowing treatment likely stems from induced damage to the muscle cells resulting from increased exertion, a phenomenon common in MD (Ozawa *et al.* 1999; Petrof *et al.* 1993; Sander *et al.* 2000; Sussman 2002). By raising worms in forced burrowing conditions, research related to MD in *C. elegans* will likely benefit from the more dramatic extent of cell death (few vs. most muscle cells), an earlier onset (by several days) and behavioral correlate (poor crawling after being raised in burrowing conditions). This approach has an additional benefit over traditional ones where a sensitizing mutation is introduced to exacerbate the *dys-1* phenotype (Giugia *et al.* 1999) because potential treatments, whether genetic or pharmacological, may be masked by the severity of the sensitizing mutation.

Muscle degeneration in *dys-1* mutants was accompanied by a decrease in intensity of fluorescence of GFP-tagged mitochondria and nuclei (Fig. 5a). This may relate to a general decline in muscle protein production and/or increase in protein degradation. Alternatively, because the *dys-1* mutant worms were defective in burrowing, they may have had less access to food at the other end of the pipette, and consequently been deprived of food. Starvation is known to induce organism-wide changes in protein processing, including autophagy (Kang *et al.* 2007). Thus, the dim GFP might also be explained by increased autophagy. Future work may compare the relative change in fluorescence in different tissues to resolve whether the *dys-1* mutation leads to specific loss of muscle proteins.

Our suppressor screen resulted in four isolated strains that (with varying success) rescued the ability of *dys-1* mutant worms to burrow (Fig. 6a). Further characterization of these strains may yield useful genetic loci for the treatment of the debilitating effects of MD, a fatal degenerative disease that affects 1 in 3,500 live male births (Davies & Nowak 2006; Goldstein & McNally 2010).

Aside from its translational advantages, burrowing is an important natural behavior common to free-living and parasitic organisms, both terrestrial and aquatic. Understanding the neural and genetic basis of burrowing will shed light on a form of locomotion employed by most animal life on the planet.

References

Bargmann, C.I. & Horvitz, H.R. (1991) Chemosensory neurons with overlapping functions direct chemotaxis to multiple chemicals in *C. elegans*. *Neuron* **7**, 729–742.

Brenner, S. (1974) The genetics of *Caenorhabditis elegans*. *Genetics* **77**, 71–94.

Croll, N.A. (1975) Components and patterns of in the behavior of the nematode *Caenorhabditis elegans*. *J Zool* **176**, 159–176.

Culetto, E. & Sattelle, D.B. (2000) A role for *Caenorhabditis elegans* in understanding the function and interaction of human disease genes. *Hum Mol Gen* **9**, 869–877.

Davies, K.E. & Nowak, K.J. (2006) Molecular mechanisms of muscular dystrophies: old and new players. *Nat Rev Mol Cell Biol* **7**, 762–773.

Deconinck, A.E., Rafael, J.A., Skinner, J.A., Brown, S.C., Potter, A.C., Metzinger, L., Watt, D.J., Dickson, J.G., Tinsley, J.M. & Davies, K.E. (1997) Utrophin-dystrophin-deficient mice as a model for Duchenne muscular dystrophy. *Cell* **90**, 717–727.

Dorgan, K.M. (2008) Worms as wedges: effects of sediment mechanics on burrowing behavior. *J Mar Res* **66**, 219–254.

Dougherty, E.C. & Calhoun, H.G. (1948) Possible significance of free-living nematodes in genetic research. *Nature* **161**, 29.

Durbeej, M. & Campbell, K.P. (2002) Muscular dystrophies involving the dystrophin-glycoprotein complex: an overview of current mouse models. *Curr Opin Genet Dev* **12**, 349–361.

Gieseler, K., Grisoni, K. & Ségalat, L. (2000) Genetic suppression of phenotypes arising from mutations in dystrophin-related genes in *Caenorhabditis elegans*. *Curr Biol* **10**, 1092–1097.

Giuglia, J., Gieseler, K., Arpagaus, M., & Ségalat, L. (1999) Mutations in the dystrophin-like *dys-1* gene of *Caenorhabditis elegans* result in reduced acetylcholinesterase activity. *FEBS Lett* **463**, 270–272.

Goldstein, J.A. & McNally, E.M. (2010) Mechanisms of muscle weakness in muscular dystrophy. *J Gen Physiol* **136**, 29–34.

Harris, H.E. & Epstein, H.F. (1977) Myosin and paramyosin of *Caenorhabditis elegans*: biochemical and structural properties of wild-type and mutant proteins. *Cell* **10**, 709–719.

Hart, A.C. (ed.) (2006) Behavior. (July 3, 2006), *WormBook*, ed. The C. elegans Community, Wormbook, doi/10.1895/wormbook.1.87.1, http://www.wormbook.org

Iino, Y. & Yoshida, K. (2009) Parallel use of two behavioral mechanisms for chemotaxis in *Caenorhabditis elegans*. *J Neurosci* **29**, 5370–5380.

Jorgensen, E.M. & Mango, S.E. (2002) The art and design of genetic screens: *Caenorhabditis elegans*. *Nat Rev Genet* **3**, 356–369.

Kaletta, T. & Hengartner, M.O. (2006) Finding function in novel targets: *C. elegans* as a model organism. *Nat Rev Drug Discov* **5**, 387–399.

Kang, C., You, Y.J. & Avery, L. (2007) Dual roles of autophagy in the survival of *Caenorhabditis elegans* during starvation. *Genes Dev* **21**, 2161–2171.

Kim, H., Pierce-Shimomura, J.T., Oh, H.J., Johnson, B.E., Goodman, M.B. & McIntire, S.L. (2009) The dystrophin complex controls BK channel localization and muscle activity in *Caenorhabditis elegans*. *PLoS Genet* **5**, e1000780. DOI:10.1371/journal.pgen.1000780.

Kucherenko, M.M., Pantoja, M., Yatsenko, A.S., Shcherbata, H.R., Fischer, K.A., Maksymiv, D.V., Chernyk, Y.I. & Ruohola-Baker, H. (2008) Genetic modifier screens reveal new components that interact with the Drosophila dystroglycan complex. *Plos ONE* **3**, e2418.

Mariol, M.C., Ségalat, L. Muscular degeneration in the absence of dystrophin is a calcium-dependent process. *Curr Biol* **11**, 1691–1694.

McIntire, S.L., Reimer, R.J., Schuske, K., Edwards, R.H. & Jorgensen, E.M. (1997) Identification and characterization of the vesicular GABA transporter. *Nature* **389**, 870–876.

Michele, D.E., Barresi, R., Kanagawa, M., Saito, F., Cohn, R.D., Satz, J.S., Dollar, J., Nishino, I., Kelley, R.I., Somer, H., Straub, V., Mathews, K.D., Moore, S.A. & Campbell, K.P. (2002) Post-translational disruption of dystroglycan-ligand interactions in congenital muscular dystrophies. *Nature* **418**, 417–422.

Monaco, A.P., Neve, R.L., Colletti-Feener, C., Bertelson, C.J., Kurnit, D.M. & Kunkel, L.M. (1986) Isolation of candidate cDNAs for portions of the Duchenne muscular dystrophy gene. *Nature* **323**, 646–650.

Moore, S.A., Saito, F., Chen, J., Michelle, D.E., Henry, M.D., Messing, A., Cohn, R.D., Ross-Barta, S.E., Westra, S., Williamson, R.A., Hoshi, T. & Campbell, K.P. (2002) Deletion of brain dystroglycan recapitulates aspects of congenital muscular dystrophy. *Nature* **418**, 422–425.

Oh, K.H. & Kim, H. (2013) Reduced IGF signaling prevents muscle cell death in a *Caenorhabditis elegans* model of muscular dystrophy. *Proc Natl Acad Sci USA* **110**, 19024–19029.

Ozawa, E., Hagiwara, Y. & Yoshida, M. (1999) Creatine kinase, cell membrane and Duchenne muscular dystrophy. *Mol Cell Biochem* **190**, 143–151.

Petrof, B.J., Shrager, J.B., Stedman, H.H., Kelly, A.M. & Sweeney, H.L. (1993) Dystrophin protects the sarcolemma from stresses developed during muscle contraction. *Proc Natl Acad Sci USA* **90**, 3710–3714.

Pierce-Shimomura, J.T., Morse, T.M. & Lockery, S.R. (1999) The fundamental role of pirouettes in *Caenorhabditis elegans* chemotaxis. *J Neurosci* **19**, 9557–9569.

Pierce-Shimomura, J.T., Chen, B.L., Mun, J.J., Ho, R., Sarkis, R. & McIntire, S.L. (2008) Genetic analysis of crawling and swimming locomotory patterns in *C. elegans*. *Proc Natl Acad Sci USA* **105**, 20982–20987.

Sander, M., Chavoshan, B., Harris, S.A., Iannaccone, S.T., Stull, J.T., Thomas, G.D. & Victor, R.G. (2000) Functional muscle ischemia in neuronal nitric oxide synthase-deficient skeletal muscle of children with Duchenne muscular dystrophy. *Proc Natl Acad Sci USA* **97**, 13818–13823.

Shcherbata, H.R., Yatsenko, A.S., Patterson, L., Sood, V.D., Nudel, U., Yaffe, D., Baker, D. & Ruohola-Baker, H. (2007) Dissecting muscle and neuronal disorders in a Drosophila model of muscular dystrophy. *EMBO J* **26**, 481–493.

Sussman, M. (2002) Duchenne muscular dystrophy. *J Am Acad Orthop Surgeons* **10**, 138–151.

Timmons, L. & Fire, A. (1998) Specific interference by ingested dsRNA. *Nature* **29**, 854.

Torres, L.F. & Duchen, L.W. (1987) The mutant mdx: inherited myopathy in the mouse. Morphological studies of nerves, muscles and end-plates. *Brain* **110**, 269–299.

Vidal-Gadea, A.G., Davis, S., Becker, L. & Pierce-Shimomura, J.T. (2012) Coordination of behavioral hierarchies during environmental transitions in *Caenorhabditis elegans*. *Worm* **1**, 5–11.

Ward, S. (1973) Chemotaxis by the nematode *Caenorhabditis elegans*: identification of attractants and analysis of the response by use of mutants. *Proc Natl Acad Sci USA* **70**, 817–821.

Acknowledgments

We are grateful to Dr Hongkyun Kim for donated strains. Some strains were provided by the Caenorhabditis Genetic Center, which is funded by NIH Office of Research Infrastructure Programs (P40 OD010440). This study was funded by The University of Texas at Austin Undergraduate Research Award to C.B. and grant (NS075541) from NIH NINDS to J.T.P.-S. The authors declare no competing financial interests.

Supporting Information

Additional supporting information may be found in the online version of this article at the publisher's web-site:

Figure S1: Dampening of bends. The maximal amplitude of body bends decreases in amplitude when propagating from neck to tail more for swimming and crawling than

for burrowing. Quantification for bend dampening shown at bottom where ** represents $P < 0.001$ and bars SEM $N = 8$ for each group.

Figure S2: Lack of functional DYS-1 protein impairs burrowing but not the ability to tax toward a stimulus. (a) *dys-1* mutants migrated across a 10-cm agar plate toward a 2-μl diacetyl (1:100 dilution) droplet as well as wild-type animals (5 assays and >350 animals for each condition). (b) Two tested *dys-1* alleles were similarly impaired at burrowing. To eliminate the possibility of a background mutation being responsible for their inability to burrow, we fed RNAi bacteria to wild-type animals, which contained either an empty vector (RNAi ctrl) or *dys-1* RNAi. Worms where *dys-1* was selectively knocked down displayed a similar burrowing impairment as the mutant alleles.

Figure S3: Dystrophin-independent disruption of the dystrophin complex impairs burrowing in *C. elegans*. (a) To test if disrupting other proteins involved in the dystrophin muscle complex could similarly impair burrowing in worms, we assessed the burrowing ability of *islo-1* worms. Similar to *dys-1* mutants, *islo-1* animals could crawl normally but were impaired at burrowing (b).

Figure S4: *dys-1* suppressor partially rescues muscle degeneration induced by burrowing. To quantify the partial rescue observed by *dys-1*-suppressors, we counted the number of muscle nuclei observable in the midbody (a), and tail (b) of worms. (c) Sample images from midbody of worms in the three conditions. Arrowheads point at muscle nuclei. While degenerating nuclei are difficult to qualify, their dim and irregular shape is evident for *dys-1* mutants. The disruption of the muscle fibers is also indirectly evidenced by areas devoid of mitochondrial GFP, or where GFP has become aggregated.

Video S1: Burrowing behavior of *C. elegans*. A wild-type worm is shown burrowing in a glass pipette containing 3% agar.

Video S2: *Caenorhabditis elegans* burrows using lateral bends. Worms burrowing at low densities (0.5% agar) engage in lateral bends as the one shown here. During lateral bending, a dorsoventral wave is altered to move at an orthogonal plane to the original plane of locomotion.

Video S3: Worms lacking dystrophin (*dys-1*) undergo periods of immobility while burrowing. A *dys-1(eg33)* mutant worm encounters immobile sisters as it burrows in 3% agar.